

NJC

Accepted Manuscript



This is an *Accepted Manuscript*, which has been through the Royal Society of Chemistry peer review process and has been accepted for publication.

Accepted Manuscripts are published online shortly after acceptance, before technical editing, formatting and proof reading. Using this free service, authors can make their results available to the community, in citable form, before we publish the edited article. We will replace this *Accepted Manuscript* with the edited and formatted *Advance Article* as soon as it is available.

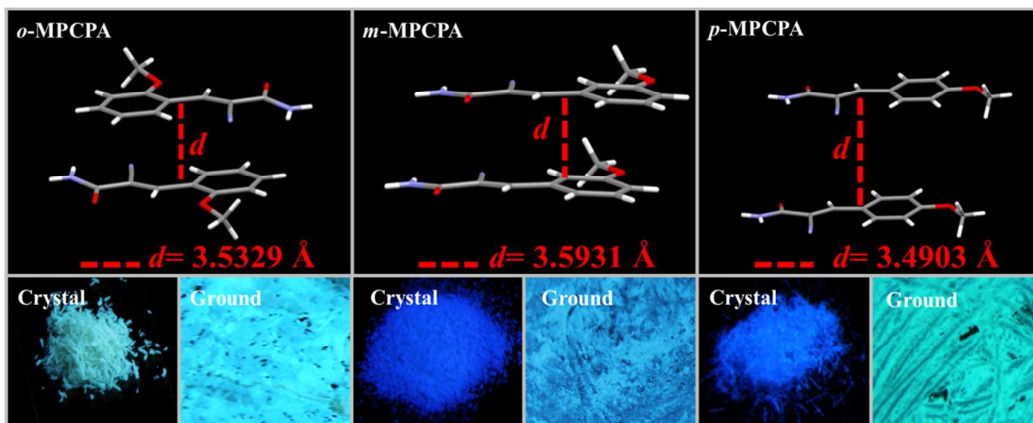
You can find more information about *Accepted Manuscripts* in the [Information for Authors](#).

Please note that technical editing may introduce minor changes to the text and/or graphics, which may alter content. The journal's standard [Terms & Conditions](#) and the [Ethical guidelines](#) still apply. In no event shall the Royal Society of Chemistry be held responsible for any errors or omissions in this *Accepted Manuscript* or any consequences arising from the use of any information it contains.



www.rsc.org/njc

Graphical abstract



Three structural-simple 3-aryl-2-cyano acrylamide derivatives (o-MPCPA, m-MPCPA and p-MPCPA) were synthesized, which exhibited the different optical properties due to the distinct face-to-face stacking mode.

ARTICLE

Effect of Stacking Mode on Mechanofluorochromic Properties of 3-Aryl-2-Cyano Acrylamide Derivatives

Cite this: DOI: 10.1039/x0xx00000x

Qingbao Song,^a Yongsheng Wang,^a Chenchen Hu,^b Yujian Zhang,^{b*} Jingwei Sun,^a Kunyan Wang,^b and Cheng Zhang^{a*}

Received 00th January 2012,
Accepted 00th January 2012

DOI: 10.1039/x0xx00000x

www.rsc.org/

Three structural-simple 3-aryl-2-cyano acrylamide derivatives, 2-cyano-3-(2-methoxyphenyl)-2-propenamide (1), 2-cyano-3-(3-methoxyphenyl)-2-propenamide (2) and 2-cyano-3-(4-methoxyphenyl)-2-propenamide (3) were synthesized. They exhibited different optical properties due to the distinct face-to-face stacking mode. The as-prepared crystals of 1 exhibited green luminescence and its emission peak did not change after grinding treatment. However, the emission peak of 2 ($\Phi_f = 12\%$) and 3 ($\Phi_f = 16\%$) exhibited an obvious red-shift upon grinding, and their corresponding quantum yields were decreased to 8% and 10%, respectively. Following the differential scanning calorimetry the Powder X-ray diffractometry data indicated that the optical properties of the 2 and 3 could be attributed to the transformation from the crystalline phase to the amorphous phase. X-Ray crystal structure, Infrared Spectroscopy and the fluorescence lifetime experiments data further validated the relationship among fluorescence switching, stacking mode and molecular interactions.

Introduction

Mechanochromic fluorescent (MCF) materials revealing reversible fluorescent changes under external force stimuli,¹ could be applied to sensors, memory chips and security inks.² Recently, rapid development has been achieved in the materials systems and the formation mechanism of MCF behaviours. Take mechanism for instance, the luminophores with the highly twisted conformation were reported recently,³⁻⁵ whose molecular structure adopted a more planar conformation after grinding that induced a longer wavelength. In addition, the excitonic interaction was substantially altered in accord with various stacking modes, where excimer formation resulted in the redshift of fluorescence.⁶ Up to date, the overwhelming majority of MCF materials exhibited the phase transformation from the crystalline state to (partial) amorphous state.⁷ However, there is some doubt about whether the organic powders with phase transition will reveal MCF behaviours. Thus, it is still essential to further understand the relationship between the molecular packing characteristics and the resulting MCF properties at the molecular-level.

Recently, Yang's group reported that 9,10-bis(alkoxystyryl)-anthracenes isomer⁸ indicated the MCF behaviours with both chain length-dependent⁹ and position-dependent. And, short alkyl-containing *o*OC3 and *m*OC3 exhibited more remarkable MCF activity than *p*OC3, which was related to molecular conformation and stacking modes. In addition, our group prepared new isomers containing the arylamine, in which changing the position of cyano group had great effects on MCF properties and packing modes¹⁰.

Clearly, employing "structural isomer" to investigate the formation mechanism of MCF properties was greatly interesting.

We have synthesized three isomers 2-cyano-3-(2-methoxyphenyl)-2-propenamide (*o*-MPCPA), 2-cyano-3-(3-methoxyphenyl)-2-propenamide (*m*-MPCPA) and 2-cyano-3-(4-methoxyphenyl)-2-propenamide (*p*-MPCPA) (in Fig 1) by a simple Knoevenagel reaction. Among them, the *m*-MPCPA and *p*-MPCPA samples with a blue fluorescence exhibited remarkable MCF properties. Its fluorescence was changed into green under the grinding treatments. For the *o*-MPCPA, the phase transition also underwent an obviously change upon grinding, but the MCF behaviour was not observed. X-Ray crystal structure and the fluorescence lifetime experiments data further validated the phase transition of MPCPA (*o*-, *m*-, *p*-). However, the intermolecular interactions remained unchanged for luminophore *o*-MPCPA, which might be the main reasons causing the "abnormal" phenomenon.

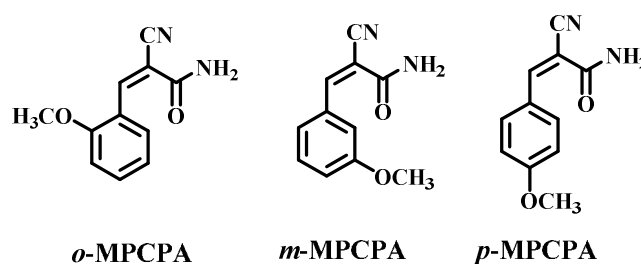


Fig 1. Molecular structures of 3-aryl-2-cyano acrylamide derivatives *o*-MPCPA, *m*-MPCP and *p*-MPCPA

Results and discussion

Single crystals of MPCPA (*o*-, *m*-, *p*-) were obtained by slow evaporation of ethanol/n-hexane mixtures. Fig. 1 exhibited the intermolecular interactions and packing modes of the neighbouring molecules. It was found that the aromatic ring, and cyano group together with the acrylamide for three MPCPA isomers were located on the same plane. For *o*-MPCPA, The crystal structure containing eight molecules in the unit cell was monoclinic with space group $I2/a$. As depicted in Fig. S2C, there were two types of hydrogen bonds between adjacent molecules with the distance of 2.379 Å and 2.113 Å respectively. The luminogens adopted the antiparallel H-type packing mode in order to fit into the crystalline lattice. From the top view, the acrylamide was directly placed above the aromatic ring of the neighbouring molecules with interplanar distance of 3.5329 Å (Fig. 2a). Importantly, the aromatic ring did not overlap between the adjacent molecules. Such antiparallel H-type packing mode didn't result in the π - π interactions, which contributed to enhance quantum yields of crystals. By comparison, the luminogens *m*-MPCPA and *p*-MPCPA involved four molecules in their unit cells. As depicted in Figs.S3C and S4C, the multiple C-H/N and C-H/O hydrogen bonds as well as H-type packing were also observed, which induced the molecular column. Interestingly, both of the luminogens *m*-MPCPA and *p*-MPCPA adopted the head-to-head or parallel arrangements. The aromatic ring was directly stacked above the benzene ring of the neighbouring molecules with inter-planar distance of 3.5931 Å and 3.4903 Å respectively (Figs. 2b and 2c). The inter-plane distance was less than the range of the effective intermolecular interaction, but π - π overlap was slightly reduced due to the slip-stacking along the long axis of the *m* (*p*)-MPCPA molecule (Figs.2b-2c)¹¹. Thus, there was a weak π - π interaction between aromatic rings, which caused fluorescence quenching.

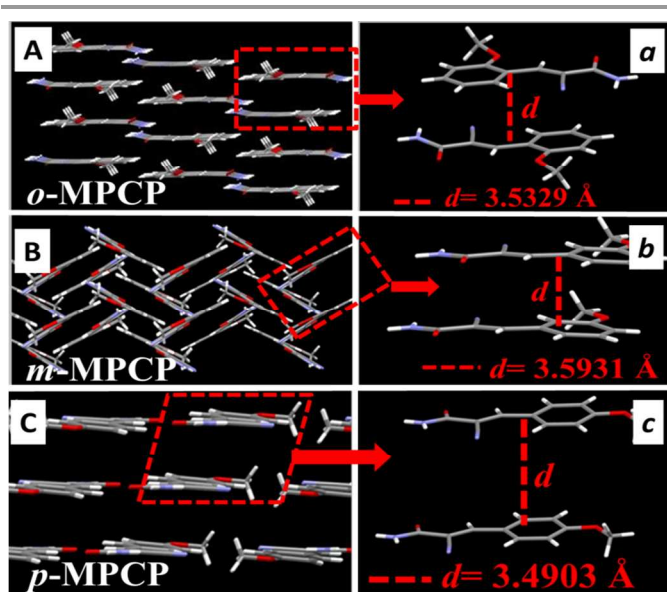


Fig.2 The packing modes and distance between the adjacent molecules in single-crystal structures of MPCPA (*o*-, *m*-, *p*-)

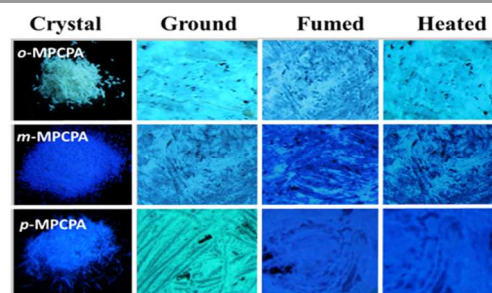


Fig.3 Fluorescence images of *o*-MPCPA, *m*-MPCP and *p*-MPCPA under a 365 nm UV light upon as-prepared, ground, fumed and heated.

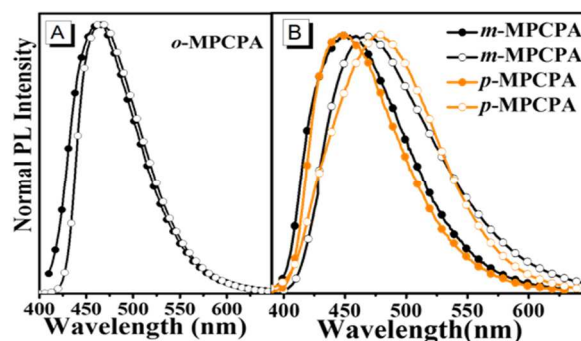


Fig.4 Fluorescence spectra of *o*-MPCPA, *m*-MPCP and *p*-MPCPA in crystal (●) and after grinding treatment (○).

In the crystalline state, the luminophore *o*-MPCPA exhibited a relatively high luminescence with quantum yields (Φ_f) of 23%. In sharp contrast, the quantum yields of *m*-MPCPA and *p*-MPCPA were decreased to 12% and 16%, respectively. As depicted in Fig. S4 and Table S1, the radiative rate constant ($k_f = \Phi_f/\tau_f$) of *o*-MPCPA was $3.7 \times 10^7 \text{ s}^{-1}$, which was similar to that of *p* (*m*)-MPCPA (approximately $4.0 \times 10^7 \text{ s}^{-1}$). However, the crystalline powders of *o*-MPCPA yielded the low non-radiative rate constant [$k_{nr} = (1-\Phi_f)/\tau_f$] of $1.2 \times 10^8 \text{ s}^{-1}$, which was increased to $3.1 \times 10^8 \text{ s}^{-1}$ for *p* (*m*)-MPCPA. The results indicated the non-radiative deactivation pathways were obviously unblocked in *m* (*p*)-MPCPA, which resulted in a lower Φ_f as a result of the weak π - π interactions. This proposal was in accordance with the head-to-head arrangements (Figs.1b-1c). Fig.3 revealed the fluorescence images of *o*-MPCPA, *m*-MPCPA and *p*-MPCPA samples upon a cycle of grinding, heating/solvent fuming. In the crystalline powders, the *o*-MPCPA with green luminescence did not exhibit MCF behaviours, because there was not an obvious spectral shift upon grinding (Fig.4A). However, the *m*-MPCPA and *p*-MPCPA samples exhibited more remarkable MCF properties (Fig.4B). The white crystals of *m*-MPCPA emitted blue-purple light ($\lambda_{\text{max}} = 452 \text{ nm}$) under the UV lights, which was changed into green ($\lambda_{\text{max}} = 470 \text{ nm}$) under the grinding treatments. Upon fuming processing with the solvent vapours such as the CH_2Cl_2 and ethyl acetate, the luminescence recovered its original state (see Fig. S6). For *p*-MPCPA, it emitted blue-purple light ($\lambda_{\text{max}} = 450 \text{ nm}$) under the UV lights, which became green ($\lambda_{\text{max}} = 478 \text{ nm}$) after grinding treatments. Clearly, MCF behaviours of MPCPA depended on the change in methoxyl position, which were in the order *p*-MPCPA > *m*-MPCPA > *o*-MPCPA.

To further investigate the MCF behaviours, differential scanning calorimetry (DSC) and powder wide-angle X-ray diffraction patterns (PXRD) of MPCPA (*o*-, *m*-, *p*-) powders in various states were performed. As depicted in Fig.S6, the ground powders of three isomers indicated an obvious cold-crystallization peak before isotropic melt transition, which did not exist in the crystal. Three obvious cold-crystallization peaks at approximately 109 °C, 85 °C and 132 °C were observed for the ground samples of *o*-MPCPA, *m*-MPCP and *p*-MPCPA, respectively. In previous report, the existence of the cold-crystallization peak indicated the ground powders were a metastable state transforming into a more stable packing structure via annealing, which was related to the MCF behaviours. However, in our case, the *o*-MPCPA samples did not exhibit MCF properties even though the ground *o*-MPCPA solids showed an evident cold-crystallization peak (Fig. S7A). Powder X-ray diffraction patterns showed that the pristine powders of dyes MPCPA obviously exhibited the numerous sharp and intense reflection peaks, which indicated a well-defined microcrystalline structure. These peaks of the MPCPA samples almost disappeared and became weak, broad and diffused peaks upon grinding. The results showed that the crystal lattice was significantly disrupted and a new amorphous phase was formed (Fig. 5). The ground samples could be recovered to the original states after solvents or heating treatment. Thus, the MCF properties of *m* (*p*)-MPCPA could be

attributed to the transformation from the crystalline phase to the amorphous phase, which coincided with the previous results.⁷ Conspicuously, the evident phase transition of *o*-MPCPA sample which did not produced the MCF behaviours was also observed. What were the reasons causing the “abnormal” phenomenon?

IR spectra of *o*-MPCPA powders were identical before and after grinding (Fig. 6A). In contrast, two IR peaks at 3163 and 3366 cm^{-1} ($\nu_{\text{N-H}}$) existed in the luminogens *m*-MPCPA, which has disappeared upon grinding (Fig. 6B). And IR peaks at 3163 cm^{-1} ($\nu_{\text{N-H}}$) existed in the luminogens *p*-MPCPA, which had drifted upon grinding (Fig. 6C). And previously researchers usually chose a strongly twisted conjugated backbone¹²⁻¹³ as the research objects of MCF fluorophores. The disappearance and drifting of some IR peaks implied that the compound probably had more planar conformation and the stronger molecular interactions. However, we synthesized this luminogens MPCPA with the planar conformations, so that the disappearance and drifting of some IR peaks of *m*-MPCPA and *p*-MPCPA were only possibly caused by stronger molecular interactions. Thus, the disappearance and drifting of some IR peaks implied that the luminogens *m*-MPCPA and *p*-MPCPA probably contained the stronger molecular interactions than those of *o*-MPCPA in ground state.

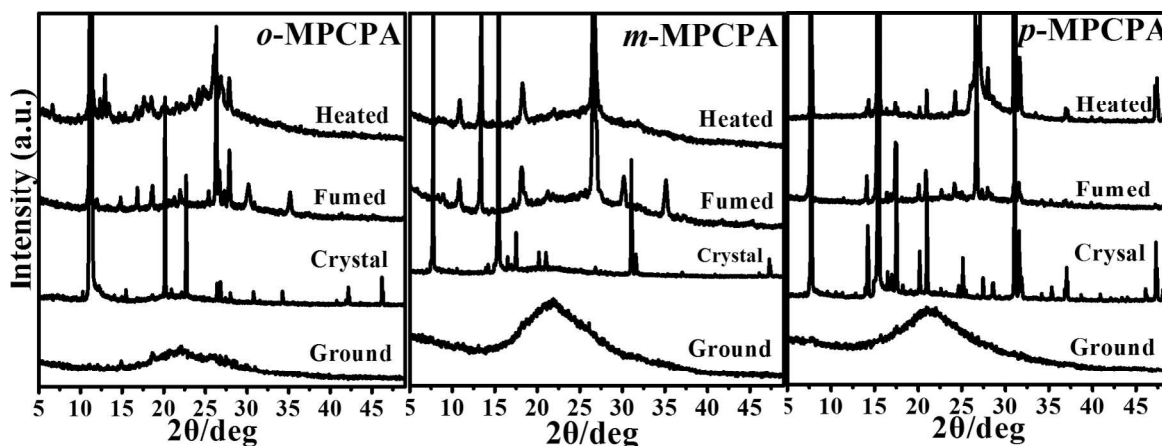


Fig. 5 PXRD profiles of *o*-MPCPA, *m*-MPCP and *p*-MPCPA powders in the different states.

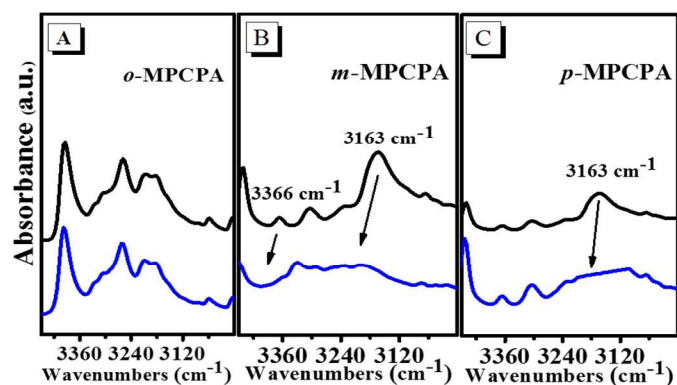


Fig.6 IR spectra of *o*-MPCPA, *m*-MPCP and *p*-MPCPA in crystals (black curve) and after grinding treatment (blue curve).

The experiment of time-resolved fluorescence further verified the proposal and the weighted mean lifetimes (τ) are illustrated in Fig. S5 and Table S1. The (τ) values of *o*-MPCPA before and after grinding were similar. By contrast, the (τ) values of *m*-MPCPA and *p*-MPCPA samples in different states revealed the significant differences: 2.99 and 2.62 ns for the original samples; 4.61 and 5.22 ns for the ground samples, respectively. The increase in lifetime revealed the excitonic coupling was obviously enhanced. The as-prepared crystals of *o*-MPCPA exhibited the quantum yields (Φ_f) of 23%, which was scarcely changed upon grinding (Φ_f =24%). However, as for luminogens *m*-MPCPA (Φ_f =12%) and *p*-MPCPA (Φ_f =16%), the quantum yields were decreased to 8% and 10% upon grinding, respectively. Furthermore, the radiative rate constants (k_f) of *m*-MPCPA and *p*-MPCPA were decreased from $4.0 \times 10^7 \text{ s}^{-1}$ and $6.1 \times 10^7 \text{ s}^{-1}$ to $1.7 \times 10^7 \text{ s}^{-1}$ and $1.9 \times 10^7 \text{ s}^{-1}$ respectively. The results

indicated the π - π interaction was further enhanced, which blocked the radiative deactivation pathways, however, this process did not exist in the sample *o*-MPCPA. What were the reasons that mechanical grinding did not alter the excited state of sample *o*-MPCPA? As shown in Fig.1a, the acrylamide was placed above the aromatic ring of the neighbouring molecules. The interplanar distance was effectively reduced upon grinding, which had been demonstrated in other MCF molecules. However, the decrease in distance did not lead to the enhancing of π - π interactions. In sharp contrast, as for *m*-MPCPA and *p*-MPCPA with the head-to-head packing, the intermolecular interaction between the adjacent aromatic rings was enhanced result from the excitonic coupling. And such strong π - π interactions of the neighbouring molecules blocked the decay of the excited species through radiative pathways, resulting in the altering of excited state as well as the weak Φ_f of *m*-MPCPA (8 %) and *p*-MPCPA (10 %). Briefly, luminogen *o*-MPCPA revealed an obvious phase transition but it did not vary π - π interactions of the adjacent molecules owing to the antiparallel H-type arrangement. In a word, the luminogen *o*-MPCPA did not show the MCF properties despite the change in phase state.

Conclusions

In summary, we have synthesized the novel luminogens 3-aryl-2-cyano acrylamide derivatives (*o*-MPCPA, *m*-MPCPA and *p*-MPCPA) with differences in methoxyl position. And it was found that the optical properties and stacking mode depended on the changes in methoxyl position. The luminogens *o*-MPCPA adopted the antiparallel H-type packing mode. However, both of the luminogens *m*-MPCPA and *p*-MPCPA adopted the head-to-head or parallel arrangements. Thus, the luminogens *o*-MPCPA exhibited a relatively higher quantum yields than the luminogens *m*-MPCPA and *p*-MPCPA due to the distinct packing mode and molecular interactions. The molecular conformation and stacking modes of the luminogens MPCPA (*o*-, *m*-, *p*-) were altered under the stimulation of mechanical force. However, the luminogens *o*-MPCPA did not exhibit MCF behaviours. And for all we know, it was first example that the luminogens showed evident phase transition, which did not induce MCF behaviours. The interplanar distance was generally reduced upon grinding. However, the decrease in distance did not lead to the increasing in π - π interactions, which were the reasons causing the "abnormal" phenomenon. Thus, the MCF behaviours were not only dependent on molecular conformation and stacking modes, but also strongly related to molecular interaction.

Experimental

2-cyano-3-(2-methoxyphenyl)-2-propenamide(*o*-MPCPA), 2-cyano-3-(3-methoxyphenyl)-2-propenamide(*m*-MPCPA) and 2-cyano-3-(4-methoxyphenyl)-2-propenamide(*p*-MPCPA) were synthesized (in Chart 1) by a simple Knoevenagel reaction under gentle conditions in good yield.

A mixture of 2-(methoxy)benzaldehyde (4.08 g, 30 nmol) , 2-cyanoacetamide (2.61 g, 31 nmol) and L-Proline(0.69 g, 6 nmol) in ethanol (20 ml) was heated under reflux for 2h; the solid product was filtered, washed with ethanol, dried (91% yield) and upon

crystallization from ethanol solution gave rise to the pure product. Finally, the desired luminophore 2-cyano-3-(2-methoxyphenyl)-2-propenamide (*o*-MPCPA) were fully characterized by ^1H NMR, ^{13}C NMR and HRMS. ^1H NMR (500 MHz, CDCl_3) δ 8.81 (s, 1H), 8.19 (dd, $J = 7.8, 1.2$ Hz, 1H), 7.56 – 7.48 (dd, $J = 7.8, 1.6$ Hz, 1H), 7.07 (t, $J = 7.6$ Hz, 1H), 6.97 (d, $J = 8.5$ Hz, 1H), 6.35 (d, 2H), 3.91 (s, 3H). ^{13}C NMR (126 MHz, CDCl_3) δ 162.5, 159.3, 148.8, 134.7, 129.1, 120.9, 120.9, 117.4, 111.2, 102.7, 55.7. HRMS (ESI) Calcd. for $\text{C}_{11}\text{H}_{10}\text{N}_2\text{O}_2$ ($[\text{M}+\text{H}]^+$): 203.0821. Found: 203.0807. Crystallographic data for ***o*-MPCPA**: $\text{C}_{11}\text{H}_{10}\text{N}_2\text{O}_2$, $M = 202.21$ g mol $^{-1}$, monoclinic, $a = 13.7381(9)$ Å, $b = 8.8770(4)$ Å, $c = 17.5640(9)$ Å, $\beta = 103.368(6)^\circ$, $V = 2083.9(2)$ Å 3 , $T = 293(2)$ K, $R_{\text{int}} = 0.0214$, space group $I2/a$, $D_{\text{calc}} = 1.289$ Mg m $^{-3}$, $Z = 8$, the final R indices were $R_1 = 0.0448$, $wR_2 = 0.1153$ [$I > 2\sigma(I)$], CCDC 999360.

A mixture of 3-(methoxy)benzaldehyde (4.08 g, 30 nmol) , 2-cyanoacetamide (2.61 g, 31 nmol) and L-Proline(0.69 g, 6 nmol) in ethanol (20 ml) was heated under reflux for 2h; the solid product was filtered, washed with ethanol, dried (92% yield) and upon crystallization from ethanol solution gave rise to the pure product. Finally, the desired luminophore 2-cyano-3-(3-methoxyphenyl)-2-propenamide (*o*-MPCPA) were fully characterized by ^1H NMR, ^{13}C NMR and HRMS. ^1H NMR (500 MHz, CDCl_3) δ 8.31 (s, 1H), 7.54-7.48 (m, 2H), 7.42 (t, $J = 7.8$ Hz, 1H), 7.11– 7.09 (m, 1H), 6.43 (s, 1H), 6.19 (s, 1H), 3.87 (s, 3H). ^{13}C NMR (126 MHz, CDCl_3) δ 162.1, 160.0, 154.1, 132.8, 130.3, 123.8, 119.7, 117.1, 114.6, 103.3, 55.4. HRMS (ESI) Calcd. for $\text{C}_{11}\text{H}_{10}\text{N}_2\text{O}_2$ ($[\text{M}+\text{H}]^+$): 203.0821. Found: 203.0822. Crystallographic data for ***m*-MPCPA**: $\text{C}_{11}\text{H}_{10}\text{N}_2\text{O}_2$, $M = 202.21$ g mol $^{-1}$, monoclinic, $a = 15.6778(10)$ Å, $b = 3.9598(3)$ Å, $c = 17.4076(14)$ Å, $\beta = 108.928(8)^\circ$, $V = 1022.26(13)$ Å 3 , $T = 293(2)$ K, $R_{\text{int}} = 0.0235$, space group $P2(1)/c$, $D_{\text{calc}} = 1.314$ Mg m $^{-3}$, $Z = 4$, the final R indices were $R_1 = 0.0430$, $wR_2 = 0.1138$ [$I > 2\sigma(I)$], CCDC 999359.

A mixture of 4-(methoxy)benzaldehyde (4.08 g, 30 nmol) , 2-cyanoacetamide (2.61 g, 31 nmol) and L-Proline(0.69 g, 6 nmol) in ethanol (20 ml) was heated under reflux for 2h; the solid product was filtered, washed with ethanol, dried (94% yield) and upon crystallization from ethanol solution gave rise to the pure product. Finally, the desired luminophore 2-cyano-3-(4-methoxyphenyl)-2-propenamide (*o*-MPCPA) were fully characterized by ^1H NMR, ^{13}C NMR and HRMS. ^1H NMR (500 MHz, DMSO) δ 8.11 (s, 1H), 7.97 (d, $J = 8.8$ Hz, 2H), 7.79 (s, 1H), 7.72 – 7.59 (m, 1H), 7.14 (t, $J = 5.8$ Hz, 2H), 3.86 (s, 3H). ^{13}C NMR (126 MHz, DMSO) δ 163.1, 162.6, 150.1, 132.4, 124.4, 117.0, 114.8, 102.9, 55.6, 54.7. HRMS (ESI) Calcd. for $\text{C}_{11}\text{H}_{10}\text{N}_2\text{O}_2$ ($[\text{M}+\text{H}]^+$): 203.0821. Found: 203.0824. Crystallographic data for ***p*-MPCPA**: $\text{C}_{11}\text{H}_{10}\text{N}_2\text{O}_2$, $M = 202.21$ g mol $^{-1}$, monoclinic, $a = 3.920(2)$ Å, $b = 10.792(6)$ Å, $c = 23.124(12)$ Å, $\beta = 93.463(8)^\circ$, $V = 976.5(9)$ Å 3 , $T = 293(2)$ K, $R_{\text{int}} = 0.1143$, space group $P2(1)/c$, $D_{\text{calc}} = 1.375$ Mg m $^{-3}$, $Z = 4$, the final R indices were $R_1 = 0.0824$, $wR_2 = 0.2367$ [$I > 2\sigma(I)$], CCDC 999361.

Acknowledgments

The authors gratefully thank the supporting of National Natural Science Foundation of China (51403060, 51273179), National Basic Research Program of China (2011CBA00700) and International

S&T Cooperation Program, China (2012DFA-51210) and Natural Science Foundation of Zhejiang Province (LQ14B04003).

References and notes

^aState Key Laboratory Breeding Base of Green Chemistry-Synthesis Technology, College of Chemical Engineering, Zhejiang University of Technology, Hangzhou (P. R. China).

^bDepartment of Materials chemistry, Huzhou University, Xueshi Road 1#, Huzhou (P. R. China).

Corresponding Author: E-mail: czhang@zjut.edu.cn (C. Zhang); sciencezyj@foxmail.com (Y. J. Zhang)

- (a) Y. Q. Dong, J. W. Y. Lam, A. Qin, Z. Li, J. Z. Sun, H. H.-Y. Sung, I. D. Williams and B. Z. Tang, *Chem. Commun.*, 2007, 40-42; (b) B.-K. An, S. H. Gihm, J. W. Chung, C. R. Park, S.-K. Kwon and S. Y. Park, *J. Am. Chem. Soc.*, 2009, 131, 3950-3957; (c) H. Y. Zhang, Z. L. Zhang, K. Ye, J. Y. Zhang and Y. Wang, *Adv. Mater.*, 2006, 18, 2369-2372; (d) X. Fan, J. L. Sun, F. Z. Wang, Z. Z. Chu, P. Wang, Y. Q. Dong, R. R. Hu, B. Z. Tang and D. C. Zou, *Chem. Commun.*, 2008, 2989-2991.
- (a) Y. Sagara and T. Kato, *Nat. Chem.*, 2009, 1, 605-610; (b) C. Weder, Editorial, *J. Mater. Chem.*, 2011, 21, 8235-8236; (c) Z. G. Chi, X. Q. Zhang, B. J. Xu, X. Zhou, C. P. Ma, Y. Zhang, S. W. Liu and J. R. Xu, *Chem. Soc. Rev.*, 2012, 41, 3878-3896; (d) S. Hirata and T. Watanabe, *Adv. Mater.*, 2006, 18, 2725-2729; (e) S. J. Lim, B. K. An, S. D. Jung, M. A. Chung and S. Y. Park, *Angew. Chem., Int. Ed.*, 2004, 43, 6346-4350.
- (a) X. Q. Zhang, Z. G. Chi, H. Y. Li, B. J. Xu, X. F. Li, W. Zhou, S. W. Liu, Y. Zhang and J. R. Xu, *Chem.-Asian J.*, 2011, 6, 808-811; (b) X. Q. Zhang, Z. G. Chi, J. Y. Zhang, H. Y. Li, B. J. Xu, X. F. Li, S. W. Liu, Y. Zhang and J. R. Xu, *J. Phys. Chem. B*, 2011, 115, 7606-7611.
- (a) W. Z. Yuan, Y. Q. Tan, Y. Y. Gong, P. Lu, J. W. Y. Lam, X. Y. Shen, C. F. Feng, H. H. Y. Sung, Y. W. Lu, I. D. Williams, J. Z. Sun, Y. M. Zhang and B. Z. Tang, *Adv. Mater.*, 2013, 25, 2837-2843; (b) Y. Q. Dong, J. W. Y. Lam, A. J. Qin, J. X. Sun, J. Z. Liu, Z. Li, J. Z. Sun, H. H. Y. Sung, I. D. Williams, H. S. Kwok and B. Z. Tang, *Chem. Commun.*, 2007, 3255-3257.
- (a) Y. L. Wang, W. Liu, L. Y. Bu, J. F. Li, M. Zheng, D. T. Zhang, M. X. Sun, Y. Tao, S. F. Xue and W. J. Yang, *J. Mater. Chem. C*, 2013, 1, 856-862; (b) L. Y. Bu, M. X. Sun, D. T. Zhang, W. Liu, Y. L. Wang, M. Zheng, S. F. Xue and W. J. Yang, *J. Mater. Chem. C*, 2013, 1, 2028-2035; (c) W. Liu, Y. L. Wang, L. Y. Bu, J. F. Li, M. Sun, D. T. Zhang, M. Zheng, C. Yang, S. F. Xue and W. J. Yang, *J. Lumin.*, 2013, 143, 50-55.
- (a) M. J. Teng, X. R. Jia, S. Yang, X. F. Chen and Y. Wei, *Adv. Mater.*, 2012, 24, 1255-1261; (b) J. Luo, L. Y. Li, Y. L. Song and J. Pei, *Chem.-Eur. J.*, 2011, 17, 10515-10519; (c) X. Q. Zhang, Z. G. Chi, Y. Zhang, S. W. Liu and J. R. Xu, *J. Mater. Chem. C*, 2013, 1, 3376-3390.
- (a) S. Varghese and S. Das, *J. Phys. Chem. Lett.*, 2011, 2, 863-873; (b) C. Kitamura, T. Ohara, N. Kawatsuki, A. Yoneda, T. Kobayashi, H. Naito, T. Komatsuc and T. Kitamura, *CrystEngComm*, 2007, 9, 644-647; (c) H. Y. Zhang, Z. L. Zhang, K. Q. Ye, J. Y. Zhang and Y. Wang, *Adv. Mater.*, 2006, 18, 2369-2372; (d) R. R. Wei, P. S. Song and A. J. Tong, *J. Phys. Chem. C*, 2013, 117, 3467-3474; (e) T. Mutai, H. Satou and K. Araki, *Nat. Mater.*, 2005, 4, 685-687; (f) S. P. Anthony, *ChemPlusChem*, 2012, 77, 518-531. (g) X. Q. Zhang, Z. G. Chi, B. J. Xu, C. J. Chen, X. Zhou, Y. Zhang, S. W. Liu and J. R. Xu, *J. Mater. Chem.*, 2012, 22, 18505-18513;
- W. Liu, Y. L. Wang, M. X. Sun, D. T. Zhang, M. Zheng and W. J. Yang, *Chem. Commun.*, 2013, 49, 6042-6044.
- (a) X. Q. Zhang, Z. G. Chi, B. R. Xu, L. Jiang, X. Zhou, Y. Zhang, S. W. Liu and J. R. Xu, *Chem. Commun.*, 2012, 48, 10895-10897; (b) X. Q. Zhang, Z. G. Chi, X. Zhou, S. W. Liu, Y. Zhang and J. R. Xu, *J. Phys. Chem. C* 2012, 116, 23629-23638
- Y. J. Zhang, G. L. Zhuang, M. Ouyang, B. Hu, Q. B. Song, J. W. Sun, C. Zhang, C. Gu, Y. X. Xu and Y. G. Ma, *Dyes Pigments*, 2013, 98, 486-492.
- (a) S. J. Yoon, J. W. Chung, J. Gierschner, K. S. Kim, M. G. Choi, D. Kim and S. Y. Park, *J. Am. Chem. Soc.*, 2010, 132, 13675-13683; (b) X. Q. Zhang, Z. Y. Ma, Y. Yang, X. Y. Zhang, X. R. Jia and Y. Wei, *J. Mater. Chem. C*, 2014, DOI: 10.1039/C4TC01457J
- H. Y. Li, X. Q. Zhang, Z. G. Chi, B. J. Xu, W. Zhou, S. W. Liu, Y. Zhang and J. R. Xu, *Org. Lett.*, 2011, 13, 556-559.
- Y. J. Zhang, J. W. Sun, G. L. Zhuang, M. Ouyang, Z. W. Yu, F. Cao, G. X. Pan, P. S. Tang, C. Zhang and Y. G. Ma, *J. Mater. Chem. C*, 2014, 2, 195-200.